

# On the mass of ultra-light bosonic dark matter from galactic dynamics

V. Lora<sup>a</sup>, Juan Magaña<sup>b,1</sup>, Argelia Bernal<sup>c,1</sup>,  
F. J. Sánchez-Salcedo<sup>b,1</sup> and E. K. Grebel<sup>a</sup>

<sup>a</sup>Astronomisches Rechen-Institut, Zentrum für Astronomie der Universität Heidelberg,  
Mönchhofstr. 12-14, 69120 Heidelberg, Germany

<sup>b</sup>Instituto de Astronomía, Universidad Nacional Autónoma de México, AP 70-264, 04510  
Mexico City, Mexico

<sup>c</sup>Instituto de Ciencias Nucleares, Universidad Nacional Autónoma de México, AP 70-543,  
04510 Mexico City, Mexico

E-mail: [vlora@ari.uni-heidelberg.de](mailto:vlora@ari.uni-heidelberg.de), [jmagana@astroscu.unam.mx](mailto:jmagana@astroscu.unam.mx),  
[argelia.bernal@nucleares.unam.mx](mailto:argelia.bernal@nucleares.unam.mx), [jsanchez@astroscu.unam.mx](mailto:jsanchez@astroscu.unam.mx),  
[grebel@ari.uni-heidelberg.de](mailto:grebel@ari.uni-heidelberg.de)

**Abstract.** We consider the hypothesis that galactic dark matter is composed of ultra-light scalar particles and use internal properties of dwarf spheroidal galaxies to establish a preferred range for the mass  $m_\phi$  of these bosonic particles. We re-investigate the problem of the longevity of the cold clump in Ursa Minor and the problem of the rapid orbital decay of the globular clusters in Fornax and dwarf ellipticals. Treating the scalar field halo as a rigid background gravitational potential and using  $N$ -body simulations, we have explored how the dissolution timescale of the cold clump in Ursa Minor depends on  $m_\phi$ . It is demonstrated that for masses in the range  $0.3 \times 10^{-22} \text{ eV} < m_\phi < 1 \times 10^{-22} \text{ eV}$ , scalar field dark halos without self-interaction would have cores large enough to explain the longevity of the cold clump in Ursa Minor and the wide distribution of globular clusters in Fornax, but small enough to make the mass of the dark halos compatible with dynamical limits. It is encouraging to see that this interval of  $m_\phi$  is consistent with that needed to suppress the overproduction of substructure in galactic halos and is compatible with the acoustic peaks of cosmic microwave radiation. On the other hand, for self-interacting scalar fields with coupling constant  $\lambda$ , values of  $m_\phi^4/\lambda \lesssim 0.55 \times 10^3 \text{ eV}^4$  are required to account for the properties of the dark halos of these dwarf spheroidal galaxies.

**Keywords:** dark matter theory, dark matter simulations, dwarf galaxies

---

<sup>1</sup>Part of the Instituto Avanzado de Cosmología (IAC) collaboration <http://www.iac.edu.mx/>

---

## Contents

<b>1</b>	<b>Introduction</b>	<b>1</b>
<b>2</b>	<b>The Schrödinger-Poisson System</b>	<b>2</b>
<b>3</b>	<b>The halo of UMi dSph: Constraints on SFDM</b>	<b>5</b>
3.1	The dark halo and the dynamical fossil in UMi	5
3.2	Scalar field without self-interaction ( $\Lambda = 0$ )	6
3.2.1	Upper limit on $m_\phi$	6
3.2.2	Lower limit on $m_\phi$	8
3.3	Scalar field with self-interaction ( $\Lambda \neq 0$ )	9
3.3.1	Small $\Lambda$ -values ( $\Lambda \approx 1$ )	9
3.3.2	Large $\Lambda$ -values ( $\Lambda \gg 1$ )	10
<b>4</b>	<b>The halo of Fornax and the orbital decay of GCs</b>	<b>11</b>
<b>5</b>	<b>Concluding Remarks</b>	<b>15</b>
<b>6</b>	<b>Acknowledgments</b>	<b>17</b>
<b>A</b>	<b>Wake created by a gravitational perturber in an infinite homogeneous medium</b>	<b>17</b>

---

## 1 Introduction

The Concordance Cosmological Model, usually referred to as the  $\Lambda$ + cold dark matter ( $\Lambda$ CDM) model, has proved to be very successful in explaining observables across a wide range of length scales, from the cosmic microwave background (CMB) anisotropy to the Lyman- $\alpha$  forest. In this model, nonbaryonic collisionless cold dark matter (hereafter CDM) makes up 23% of the total mass content of the Universe.

Observational data on galactic scales seem to disagree with CDM predictions. High resolution  $N$ -body simulations have shown that the predicted number of subhalos is an order of magnitude larger than what has been observed [1, 2]. Another discrepancy arises when comparing the density profiles of dark halos predicted in simulations with those derived from observations of dwarf spheroidal (dSph) galaxies and Low Surface Brightness galaxies (LSB's);  $N$ -body simulations predict an universal cuspy density profile, while observations indicate that a cored halo is preferred in an important fraction of low-mass galaxies [3–5].

These discrepancies might be overcome by considering other alternatives. One intriguing possibility is to consider DM particles as spin zero bosons of ultra-light mass  $m_\phi$ , having such a large Compton wavelength and a very large number density that they can be described by a classical scalar field  $\phi$  (hereafter Scalar Field Dark Matter; SFDM) [6–20]. In this scenario the massive scalar field only interacts gravitationally with the rest of the matter and is minimally coupled to gravity. Different potentials have been proposed to the scalar field, e.g.  $V(\Phi) = V_0 [\cosh(\xi\Phi) - 1]$  [13],  $V(\Phi) = m_\phi^2 \Phi^2/2$  [21, 22] and  $V(\Phi) = m_\phi^2 \Phi^2/2 + \lambda \Phi^4/4$  [20]. At cosmological scales, it is well known that if the quadratic term of  $V_\phi$  is dominant, the SFDM behaves as CDM and thus linear perturbations of SFDM evolve as those in the

standard CDM paradigm [20–22]. However, a difference between SFDM and CDM models is that a cut-off in its mass power spectrum, which can prevent the overproduction of substructures, naturally arises in SFDM. For a quadratic potential, the substructure overproduction issue could be overcome if the boson associated to the scalar field is ultra-light with a mass of  $m_\phi \sim 10^{-23} - 10^{-22}$  [10, 13]. It is important to note that an ultra-light bosonic DM particle of mass  $\sim 1 \times 10^{-22}$  eV is compatible with the acoustic peaks of the CMB radiation [23].

On the other hand, it has been shown that the scalar field can form stable structures that could account for DM halos [24]. It is known [25–31] that ground states are stable against spherical and non-spherical perturbations and, furthermore, that such configurations are late-time attractors for quite arbitrary initial profiles of the scalar field [31]. These findings suggest that ground states could be naturally formed from initial fluctuations of the hypothetical SFDM.

Interestingly, SFDM halos would have cored mass density profiles. Arbey, Lesgourgues & Salati [14] have analyzed the rotation curves in a sample of LSB galaxies with SFDM and conclude that ground states can explain fairly well the observed rotation curves, if the mass of the boson is  $m_\phi \sim 10^{-24} - 10^{-23}$  eV (see also [6, 32–34]). If the scalar field is self-interacting, its mass  $m_\phi$  and its self-coupling parameter  $\lambda$  are both constrained in order to fit the rotation curves of spiral galaxies [35–38]. The dynamics of head-on collisions of ground state halos have been also studied [39, 40].

Here we consider the DM halos of dSph galaxies in the context of SFDM. Our aim is to provide new constraints on SFDM assuming that it behaves as a massive and complex scalar field. We will discuss cases with and without self-interaction. dSph galaxies provide a unique testing ground for the nature of DM. There is growing evidence that Ursa Minor (UMi), Fornax, Sculptor, Carina, Leo I and Leo II possess cored DM halos instead of cuspy [4, 41–45]. It is worthwhile exploring if the SFDM scenario can explain the existence of cores in dSph galaxies and circumvent some problems in galactic dynamics in a natural way. Here we investigate two of these problems. First of all, we argue that the interpretation that the stellar clump in UMi is a ‘dynamical fossil’ gives constraints on  $m_\phi$  and  $\lambda$ . To do so, we perform  $N$ -body simulations of the evolution of a cold stellar clump embedded in the scalar field DM halo, treating it as a rigid background potential, but including clump’s self-gravity. Secondly, we argue that, for some combinations of  $m_\phi$  and  $\lambda$ , the reduction of the gravitational dynamical friction in a SFDM halo could help alleviate the problem of the orbital decay of globular clusters (GCs) in dSph galaxies and dwarf ellipticals.

The article is organized as follows. In §2 we describe the SFDM model and briefly review the Schrödinger-Poisson system. In §3, we derive constraints on the values of  $m_\phi$  by studying the puzzling internal dynamics of UMi dSph galaxy. In §4 we discuss the implications of SFDM in the Fornax dSph galaxy. Finally, in section §5 we discuss the results and give our conclusions.

## 2 The Schrödinger-Poisson System

Since galactic halos are well described as Newtonian systems, we will work within the Newtonian limit. In this limit, the Einstein-Klein-Gordon (EKG) equations for a complex scalar field  $\Phi$  minimally coupled to gravity and endowed with a potential  $V(\Phi) = m_\phi^2 \Phi^2/2 + \lambda \Phi^4/4$ ,

can be simplified to the Schrödinger-Poisson equations (SP):

$$i\hbar\partial_t\psi = -\frac{\hbar^2}{2m_\phi}\nabla^2\psi + Um_\phi\psi + \frac{\lambda}{2m_\phi}|\psi|^2\psi, \quad (2.1)$$

$$\nabla^2U = 4\pi Gm_\phi^2\psi\psi^*, \quad (2.2)$$

where  $m_\phi$  is the mass of the boson associated with the scalar field,  $U$  is the gravitational potential produced by the DM density source ( $\rho = m_\phi^2|\psi|^2$ ),  $\lambda$  is the self-interacting coupling constant, and the field  $\psi$  is related to the relativistic field  $\Phi$  through

$$\Phi = e^{-im_\phi c^2 t/\hbar}\psi, \quad (2.3)$$

[46–48].

We are interested in spherical equilibrium solutions to the SP system. They are obtained assuming harmonic temporal behavior for the scalar field

$$\psi(r, t) = e^{-i\gamma t/\hbar}\phi(r). \quad (2.4)$$

In dimensionless variables we have

$$r \rightarrow \frac{m_\phi c}{\hbar}r, \quad t \rightarrow \frac{m_\phi c^2}{\hbar}t, \quad (2.5)$$

$$\phi \rightarrow \frac{\sqrt{4\pi G\hbar}}{c^2}\phi, \quad U \rightarrow \frac{U}{c^2}, \quad \gamma \rightarrow m_\phi c^2\gamma, \quad (2.6)$$

and the stationary SP system can be written then as

$$\partial_r^2(r\phi) = 2r(U - \gamma) + 2r\Lambda\phi^3, \quad (2.7)$$

$$\partial_r^2(rU) = r\phi^2, \quad (2.8)$$

where

$$\Lambda = \frac{1}{8\pi} \frac{m_p^2}{m_\phi^2} \frac{c}{\hbar^3} \lambda, \quad (2.9)$$

and  $m_p$  is the Planck mass. In order to guarantee regular solutions, we require that the boundary conditions at  $r = 0$  are  $\partial_r U = 0$ ,  $\partial_r \phi = 0$  and  $\phi(0) = \phi_c$ , where  $\phi_c$  is an arbitrary value. On the other hand, we impose that

$$M = \int_0^\infty \phi^2 r^2 dr, \quad (2.10)$$

to be a finite number.

The system (2.7)-(2.8) can be treated as an eigenvalue problem: given a central value  $\phi_c$  and a specific value of  $\Lambda$ , there are discrete values  $\{\gamma_i\}$  for which the solutions  $\{\gamma_i, \phi_i(r), U_i(r)\}$  satisfy the boundary conditions. Solutions can be qualitatively differentiated by the number of nodes of the radial function  $\phi_i$ . The solution for which  $\phi$  has zero nodes is called the ground state. The first excited state is the name for the solution for which  $\phi$  has one node and so on. In this work, we consider only ground states because they are stable under gravitational

perturbations and thus are more suitable to model galactic halos than the unstable excited states [26].

Figure 1 shows the SFDM density profile and the gravitational potential  $U$ , as a function of radius  $r$ , for a ground state with  $\phi_c = 1$  and  $\Lambda = 0$ . In order to specify the properties of a certain halo, we will give the mass of the configuration  $M$ , and the radius  $r_{95}$ , defined as the radius of the sphere that contains 95% of the mass. In particular, the configuration in figure 1 has a mass  $M = 2.062$  and  $r_{95} = 3.799$  in dimensionless units (see Eqs. 2.5 and 2.6).

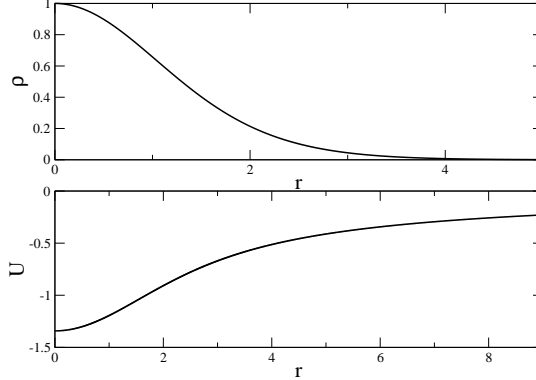


**Figure 1.** Density profile (top) and gravitational potential (bottom) of the scalar field in a ground state with  $\phi_c = 1$  and  $\Lambda = 0$ .

An interesting characteristic of the SP system is that it obeys the scaling symmetry

$$\phi, U, \gamma, \Lambda, r \rightarrow \epsilon^2 \phi, \epsilon^2 U, \epsilon^2 \gamma, \epsilon^2 \Lambda, \epsilon^{-1} r. \quad (2.11)$$

This property allows us to find a family of solutions from a particular solution. Because of this scaling symmetry, the physical quantities of the solutions satisfy

$$M, r_{95} \rightarrow \epsilon M, \epsilon^{-1} r_{95}. \quad (2.12)$$

Therefore, three quantities  $\phi_c$ ,  $m_\phi$  and  $\Lambda$  or, equivalently  $\epsilon$ ,  $m_\phi$  and  $\Lambda$  define a model completely. It is interesting that for  $\Lambda = 0$ ,  $\phi_c \sim 10^{-6}$  ( $\epsilon \sim 10^{-3}$ ) and  $m_\phi \sim 10^{-23}$  eV, the ground state would model a halo with  $M \sim 10^{10} M_\odot$ ,  $r_{95} \sim 7$  kpc, and a core radius,  $r_c$ , defined as the radius where the DM density decays a factor of 2 its central value, of  $\sim 3$  kpc.

While  $m_\phi$  and  $\lambda$  are parameters of the SFDM model that once fixed they should be universal,  $\phi_c$  (or equivalently  $\epsilon$ ) is a quantity that may vary from galaxy to galaxy. Indeed, it may be directly related to the central density of the DM halo. A typical value of  $\epsilon$  can be inferred from the (dimensionless) compactness of the ground state defined by

$$C = \frac{\epsilon^2 M}{r_{95}}. \quad (2.13)$$

Assuming that dark halos are Newtonian, it is expected that  $C \ll 1$ . This condition is fulfilled if  $\epsilon \ll 1$ . In fact, studies of general relativistic equilibrium solutions, show that

configurations with a very small central value of the scalar field  $\Phi_c$  have small values of their compactness [49]. Furthermore, it is shown that equilibrium configurations with  $\Phi_c \lesssim 10^{-6}$  can be treated as Newtonian, that is, they can be described within a good approximation by the SP system. Because of the relation (2.3), the condition  $\Phi_c \lesssim 10^{-6}$  implies  $\epsilon \lesssim 10^{-3}$ .

### 3 The halo of UMi dSph: Constraints on SFDM

UMi is a diffuse dSph galaxy located at a distance of  $69 \pm 4$  kpc [50] from the Milky Way center and has a luminosity of  $L_V = 3 \times 10^5 L_\odot$  [50]. Its stellar population is very old with an age of 10–12 Gyr. Dynamical studies suggest that UMi is a galaxy dominated by DM, with a mass-to-light ratio larger than  $60 M_\odot/L_\odot$ . Among the most puzzling observed properties of UMi is that it hosts a stellar clump, which is believed to be a dynamical fossil that survived because the underlying DM gravitational potential is close to harmonic [4, 51]. This condition is accomplished if the DM halo has a large core.

We study whether SFDM halos may have cores large enough to guarantee the survival of UMi’s clump, but small enough to ensure that the galaxy is not too massive. Indeed, models with large cores have large masses. Therefore, we have to impose an upper limit on  $V_{\max}$ , the maximum of the circular velocity of the halo. We will see that this provides a stringent constraint on the mass of the boson associated with the scalar field and on the self-interaction parameter.

#### 3.1 The dark halo and the dynamical fossil in UMi

As we said before, the most remarkable feature in UMi structure is the double off-centered density peak [52]. The second peak or clump is located on the north-eastern side of the major axis of UMi at a distance of  $\sim 0.4$  kpc from UMi’s center. The velocity distribution of the stars contained in the clump is well fitted by two Gaussians, one representing the background (velocity dispersion of  $8.8 \text{ km s}^{-1}$ ) and the other representing the velocity dispersion of the second peak ( $0.5 \text{ km s}^{-1}$ ). The most appealing interpretation is that UMi’s clump is a disrupted cluster [53] with an orbit in the plane of the sky, which has survived in phase-space because the underlying gravitational potential is harmonic [4], implying that the dark halo in UMi has a large core.

In order to explore the parameter space of galactic SFDM halos compatible with the survival of the kinematically-cold structure in UMi, we have studied the evolution of a stellar clump inside a *rigid* SFDM halo in the ground state. The dynamics of clump’s stars are simulated with 600 particles in an  $N$ -body code. Hence, a star in the clump feels the gravitational force of a static dark halo potential and the gravity of the remainder of the stars in the clump. In our simulations we ignore the contribution of the stellar background component to the gravitational potential because its mass interior to  $\sim 0.4$  kpc ( $9 \times 10^5 M_\odot$ ) only accounts about 9 percent (or less) the DM mass in UMi.

We get the gravitational potential  $U$  by solving the SP equations. In order to specify a SFDM halo we need to fix  $\epsilon$  and  $m_\phi$ . Strigari et al. [54, 55] considered dark halos compatible with the observed stellar kinematics of the classical dSph galaxies, including UMi. They found that, for realistic density profiles, the mass interior to 300 pc is  $\sim 10^7 M_\odot$  for all dSph galaxies in the Milky Way halo. Therefore, we fix the  $\epsilon$ -value in each SFDM halo by imposing that the mass within  $r = 0.39$  kpc is  $1.5 \times 10^7 M_\odot$  (see also [56–58]), and explore the evolution of the clump for halos with different  $m_\phi$ .

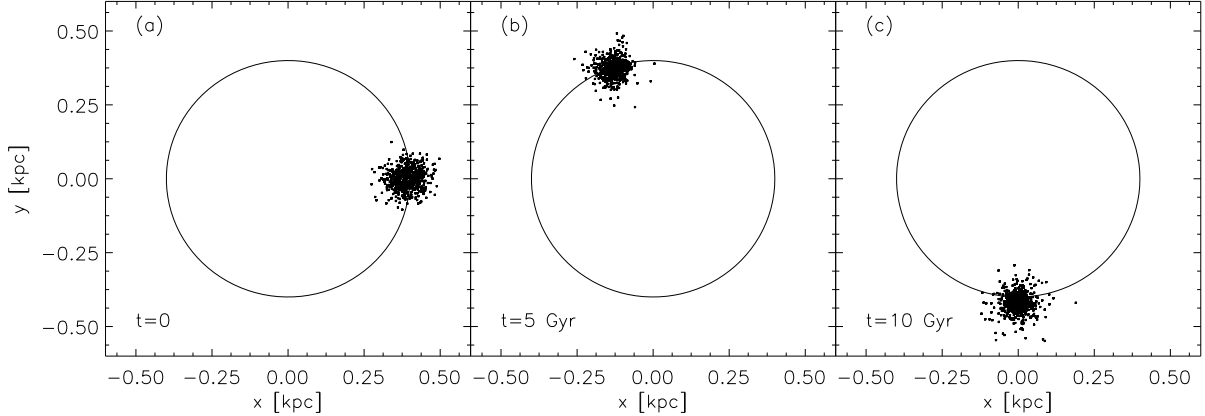


**Figure 2.** Snapshots of the clump in UMi galaxy, at  $t = 0, 5$ , and  $10$  Gyr. We set the clump on a circular orbit in the  $(x, y)$ -plane at a distance of  $r = 0.39$  kpc from UMi’s center. The mass of the boson is  $m_\phi = 10^{-23}$  eV and  $\Lambda = 0$ . The total mass of the galaxy is  $M = 9.7 \times 10^9 M_\odot$ .

Initially, the clump has a density profile  $\rho = \rho_0 \exp(-r^2/2r_0^2)$  (with  $r_0 \simeq 35$  pc [59]) and was dropped at a galactocentric distance of 0.39 kpc on a circular orbit in the  $(x, y)$  plane (see also [60]). We explored other eccentric orbits but the survival timescale is very insensitive to the eccentricity. If the  $V$ -band  $M/L$  of UMi stellar population is supposed to be  $\Upsilon_\star = 5.8$ , the mass of the clump is  $M_c = 7.8 \times 10^4 M_\odot$ . The initial one-dimensional velocity dispersion of the clump is  $1 \text{ km s}^{-1}$  [60].

The  $N$ -body simulations were performed with the code described in [51] and [60]. This  $N$ -body code has the ability to link an individual time step to each particle in the simulation. Only for the particle that has the minimum associated time, the equations of motion are integrated. This “multi-step” method reduces the typical CPU times of direct particle-particle integrations. In our simulations all the particles have the same mass and a softening length of 1 pc which is approximately 1/10th of the typical separation among clump’s particles. The convergence of the results was tested by comparing runs with different softening radii and number of particles.

### 3.2 Scalar field without self-interaction ( $\Lambda = 0$ )

#### 3.2.1 Upper limit on $m_\phi$

Figure 2 shows snapshots of the clump at  $t = 0, 5$  and  $10$  Gyr for  $m_\phi = 10^{-23}$  eV. The orbit of the clump lies in the  $(x, y)$ -plane. We see that the clump remains intact during one Hubble time. This is a consequence that the SFDM halo has a core large enough to guarantee the survival of the clump. For a mass of the boson of  $10^{-23}$  eV, the core radius is 2.4 kpc and the total halo mass of  $9.7 \times 10^9 M_\odot$ , which is too massive (see §3.2.2 for a discussion).

As the shape of the underlying gravitational potential depend on  $m_\phi$ , the longevity of the clump should depend on  $m_\phi$ . Since both the size of the core and the total mass increase when  $m_\phi$  decreases (see figure 3), we consider now the evolution of the clump in models with  $m_\phi$  values larger than  $10^{-23}$  eV. Figure 4 shows three snapshots of the clump ( $t = 0, 5$ , and  $10$  Gyr) in a halo with  $m_\phi = 10^{-22}$  eV, which has a core radius of  $\sim 0.7$  kpc. The clump does not dissolve in one Hubble time. However, when the mass of the boson is  $5 \times 10^{-22}$  eV, the core radius of the SFDM halo is quite small, of 0.28 kpc, and, consequently, the clump loses its identity due to tidal effects (see figure 5).



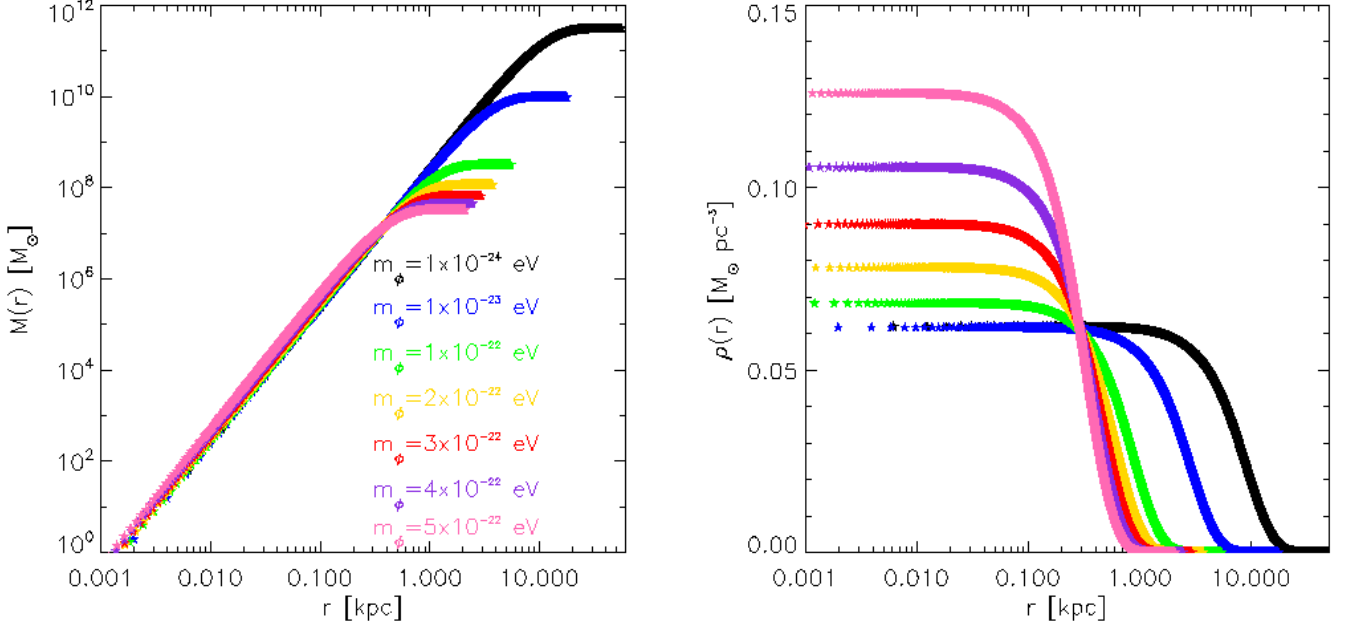


**Figure 3.** Mass interior to any given radius and density profiles for SFDM halos for models with  $\Lambda = 0$  and different  $m_\phi$ .

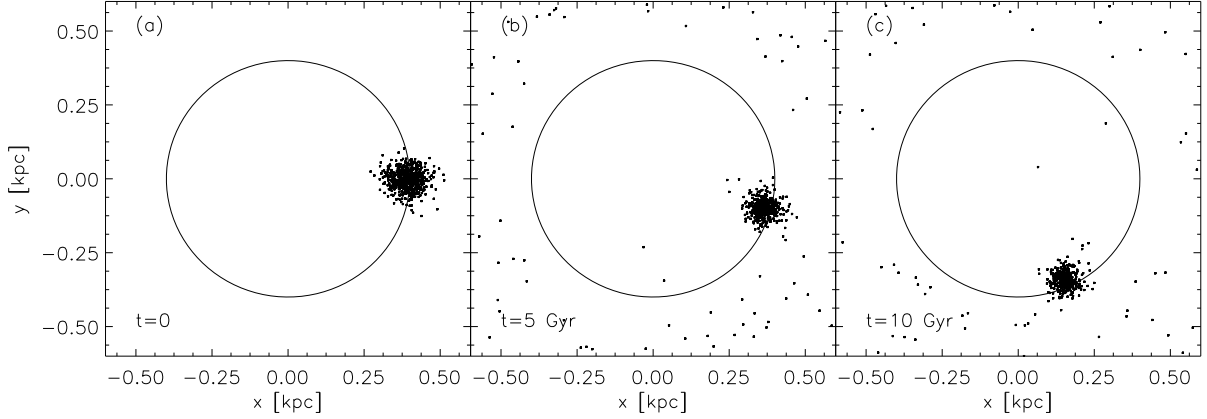


**Figure 4.** Same as figure 2 but for a boson mass of  $m_\phi = 10^{-22}$  eV and  $\Lambda = 0$ . The UMi's mass is of  $M = 3.1 \times 10^8 M_\odot$ .

To quantify the destruction of the clump in our simulations, we calculated a map of the projected surface density of mass in the  $(x, y)$ -plane at any given time  $t$  in the simulation. We sample this two-dimensional map searching for the  $10 \times 10$  pc size parcel that contains the highest mass,  $\Pi(t)$ . This parcel is centered at the remnant of the clump. Figure 6 shows the evolution of  $\Pi$  with time for models with different  $m_\phi$  and Table 1 summarizes the results of the simulations with  $\Lambda = 0$ . We see that in models with  $m_\phi \sim 3 \times 10^{-22}$  eV, the clump is diluted within one Hubble time. In halos with  $m_\phi > 3 \times 10^{-22}$  eV, the clump is erased in a too short time. Therefore, we conclude that the survival of the dynamical fossil sets an upper limit to the mass of the boson of  $m_\phi < 3 \times 10^{-22}$  eV.



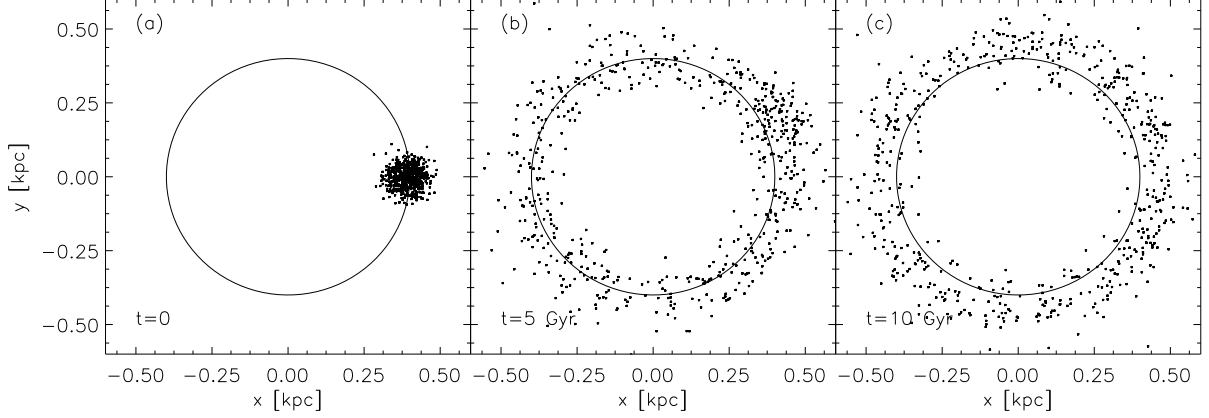


**Figure 5.** Same as figure 2 but  $m_\phi = 5 \times 10^{-22}$  eV and  $\Lambda = 0$ . In this case, the total halo mass is  $M = 0.33 \times 10^8 M_\odot$ .

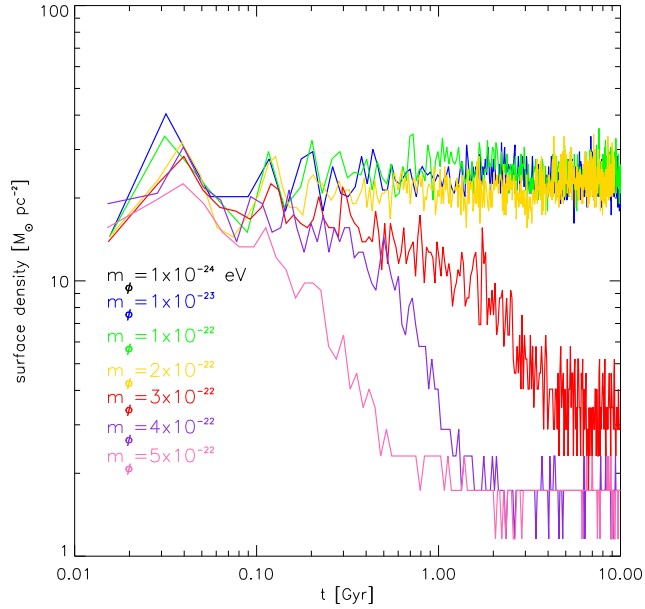


**Figure 6.** Temporal evolution of  $\Pi$  for models with  $\Lambda = 0$  and different  $m_\phi$  values.

### 3.2.2 Lower limit on $m_\phi$

In our SFDM models of UMi's halo, there is a positive correlation between the size of the core  $r_c$  and the maximum of the circular velocity  $V_{\max}$ . While large values of the core are favored to explain the persistence of the clump and are allowed by the velocity dispersion data, they require very large values of  $V_{\max}$  and  $M$ . The total mass of the halos are given in Table 1. For instance, with  $m_\phi = 10^{-23}$  eV, the total dynamical mass is  $M = 9.7 \times 10^9 M_\odot$  and  $V_{\max} \simeq 90 \text{ km s}^{-1}$ . It is extremely unlikely that one of the less luminous classical dSph galaxies has such a large mass [61]. Wilkinson et al. [56] estimate the enclosed mass of UMi within  $\sim 40'$  ( $\sim 0.8 \text{ kpc}$ ) to be of the order of  $2 \times 10^8 M_\odot$  based on projected radial velocity dispersion profiles. Peñarrubia et al. [57] suggest that the virial mass of UMi derived from

**Table 1.** Destruction times of the clump in UMi dwarf galaxy for the  $\Lambda = 0$  case, for different  $m_\phi$ . The total mass  $M$ , and the radius  $r_{95}$  and  $r_c$ , are also given for each model.

$m_\phi$ ( $10^{-22}$ eV)	$\epsilon$ ( $10^{-5}$ )	$M$ ( $10^8 M_\odot$ )	$r_{95}$ (kpc)	$r_c$ (kpc)	destruction time (Gyr)
0.01	111.0	3060	21.8	7.48	$> 10$
0.1	35.1	96.7	6.92	2.37	$> 10$
1	11.4	3.14	2.13	0.73	$> 10$
2	8.3	1.15	1.4	0.50	$> 10$
3	7.0	0.65	1.15	0.39	$\sim 5.0$
4	6.3	0.44	0.96	0.33	$\sim 1.5$
5	5.9	0.33	0.82	0.28	$\sim 0.5$

the assumption of a NFW halo model is  $\sim 4.5 \times 10^9 M_\odot$ . In fact, according to the  $\Lambda$ CDM simulations by Zentner & Bullock [62], only 5% of the subhalos in a Milky Way-sized halo has total masses  $> 5 \times 10^9 M_\odot$ . We will take this value as the upper limit on UMi mass. Note that this is a very generous upper limit for  $M$ ; fits to the velocity dispersion profile give a mass of  $2.3^{+1.6}_{-1.1} \times 10^8 M_\odot$  within a tidal radius of 1.5 kpc [54]. If we demand that  $M < 5 \times 10^9 M_\odot$ , we obtain  $m_\phi > 1.7 \times 10^{-23}$  eV, whereas for  $M < 10^9 M_\odot$  we have  $m_\phi > 5 \times 10^{-23}$  eV. Since there is evidence that at least three dSph galaxies have a dark halo with a large core (Fornax, Sculptor and UMi) and  $\Lambda$ CDM simulations have shown that it is unlikely to have a population of three subhalos with  $M \simeq 5 \times 10^9 M_\odot$  in a Milky Way-sized halo (see, e.g., [62]), a limit  $m_\phi > 3 \times 10^{-23}$  eV seems very reasonable.

Combining the above lower limit with the upper limit derived in §3.2.1, we find that  $m_\phi$  should lie between  $0.3 \times 10^{-22}$  eV to  $3 \times 10^{-22}$  eV, being our most preferred value  $m_\phi \approx 1 \times 10^{-22}$  eV. For the latter  $m_\phi$  values, the core radius of UMi dark halo is between 500 and 750 pc.

### 3.3 Scalar field with self-interaction ( $\Lambda \neq 0$ )

So far, we have assumed that boson self-interaction is negligible ( $\Lambda = 0$ ). In order to see how  $m_\phi$  depends on self-interaction, we explored models with the third term of Eq. (2.1) being distinct from zero ( $\Lambda \neq 0$ ).

#### 3.3.1 Small $\Lambda$ -values ( $\Lambda \approx 1$ )

In this section we consider small values of  $\Lambda$  (in dimensionless units). The parameters of the models are summarized in Table 2. Figures 7 and 8 show the evolution of  $\Pi(t)$  for  $\Lambda = 1/2$  and for  $\Lambda = 2$ , respectively. The halo density profiles are given in figures 9 and 10. With  $\Lambda = 1/2$ , the clump survives even if one increases the mass of the boson up to  $4 \times 10^{-22}$  eV

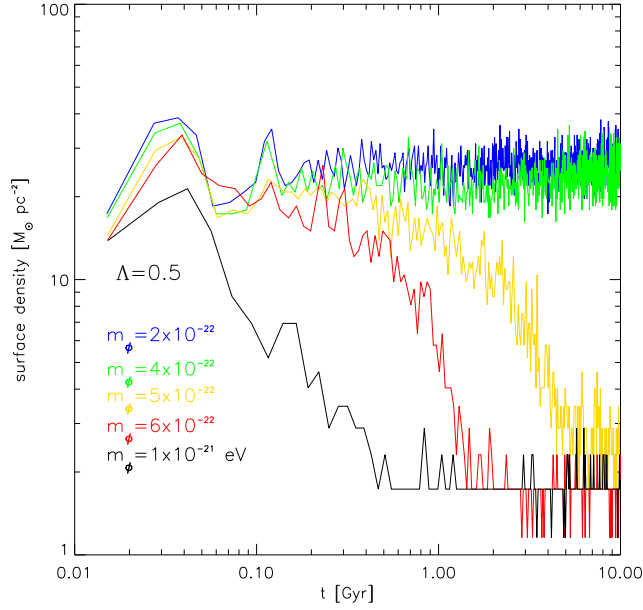


**Figure 7.** Evolution of  $\Pi$  as a function of  $t$  for a self-interaction parameter of  $\Lambda = 1/2$ .

(here the core radius is  $\sim 420$  pc). In halo models with  $m_\phi = 1 \times 10^{-21}$  eV, the clump is disrupted in  $\sim 0.4$  Gyr for  $\Lambda = 1/2$  but it survives one Hubble time for  $\Lambda = 2$ . As Table 2 shows, for the same  $m_\phi$ , the core radii of DM halos and their mass increase with  $\Lambda$ . With self-interaction, the permitted window for the mass  $m_\phi$  of the bosonic particles is shifted to larger values. We must notice, however, that in order to have  $M \gtrsim 10^8 M_\odot$ , as derived by [54],  $m_\phi \lesssim 6 \times 10^{-22}$  eV for  $\Lambda = 2$ . These constraints are compatible with those found in [63].

### 3.3.2 Large $\Lambda$ -values ( $\Lambda \gg 1$ )

Here, we analyze the effects on the persistence of the clump of UMi for large values of  $\Lambda$ . It was first pointed out in [64] that the inclusion of self-interaction, even for small values of it, can lead to important changes in the resulting scalar field configurations. In fact, from the definition of the dimensionless variable in equation (2.9), values of  $c\lambda/\hbar^3 \sim 1$  imply  $\Lambda \gg 1$ . In order to study the system of equations (2.7) and (2.8) with  $\Lambda \gg 1$ , it is useful to rescale the variables as follows:  $\phi_* = \Lambda^{1/2}\phi$  and  $r_* = \Lambda^{-1/2}r$ . In the limit  $\Lambda \rightarrow \infty$ , the Schrödinger equation (2.7), to first order in  $\Lambda^{-1}$ , has a simple algebraic form  $\phi_* = \gamma - U$ . Substituting this relation into the Poisson equation (2.8) and solving it, we obtain an exact solution for the scalar density,  $\rho_\phi = \phi^2$ , which in terms of the original variables reads as

$$\rho_\phi = \frac{\phi_c^2}{\Lambda} \frac{\sin(\Lambda^{-1/2}r)}{\Lambda^{-1/2}r}, \quad (3.1)$$

where  $\phi_c^2$  is an arbitrary constant to be determined. The condition  $\rho_\phi > 0$  provides the maximum radius  $R_{max}$  of the SFDM halo,

$$R_{max} = \pi\Lambda^{1/2}. \quad (3.2)$$

The mass profile  $M(r)$  is given by

$$M(r) = \int_0^r \phi^2 r'^2 dr' = \phi_c^2 \Lambda^{1/2} \left[ \sin \left( \Lambda^{-1/2} r \right) - \Lambda^{-1/2} r \cos \left( \Lambda^{-1/2} r \right) \right], \quad (3.3)$$

and the total halo mass  $M$  defined as the mass contained within  $R_{max}$  reads as

$$M = \pi \phi_c^2 \Lambda^{1/2}. \quad (3.4)$$

From dimensionless expressions (3.1)-(3.4), it is noticed that the free parameters of the halo are  $\Lambda$  and  $\phi_c$ . However, when the physical dimensions for those expressions are taking into account it turns out that the free parameters to fit UMi halo are  $\lambda^{1/2}/m_\phi^2$  and  $\phi_c$ . We constrain these parameters through the following steps

- assume a *reasonable* maximum UMi's radius  $R_{UMi}$ . Then, use equation (3.2) to derive  $\lambda^{1/2}/m_\phi^2$ .
- given the value of  $\lambda^{1/2}/m_\phi^2$ ,  $\phi_c$  is obtained from equation (3.3) by requiring that the mass (in units of  $m_p^2/m_\phi$ ) contained within a radius of 0.39 kpc is  $1.5 \times 10^7 M_\odot$ .
- once  $\lambda^{1/2}/m_\phi^2$  and  $\phi_c$  are known, the total halo mass and the core radius are calculated and compared with the dynamical limits discussed in §3.2.

For instance, if we take UMi's tidal radius of 1.5 kpc as the maximum radius of its halo, we obtain  $m_\phi^4/\lambda \sim 10^3 \text{ eV}^4$  ( $\hbar = c = 1$ ) and  $\phi_c^2 \sim 9.6 \times 10^{-9}$ . It follows that the total mass is  $M = 3 \times 10^8 M_\odot$  and the core radius  $r_c = 900 \text{ pc}$ . This mass is consistent with the values derived by [54], and the core radius is large enough to guarantee the survival of the clump (see tables 1 and 2). We explored different values for the tidal radius of the halo and our results are summarized in table 3. We can see that for a tidal radius of  $\sim 1.8 \text{ kpc}$ , the clump survives because the core is large enough ( $\sim 1 \text{ kpc}$ ). In this case, the SFDM halo becomes a bit more massive. On the other hand, if we impose the condition  $M > 1.5 \times 10^8 M_\odot$ , then we obtain  $m_\phi^4/\lambda < 1.7 \times 10^3 \text{ eV}^4$ .

#### 4 The halo of Fornax and the orbital decay of GCs

The fact that SFDM halos have cores might solve other apparent problems in dwarf galaxies. In this section we consider the timing problem of the orbit decay of GCs in dwarf elliptical galaxies and dSph galaxies. In fact, in a cuspy halo, GCs in these galaxies would have suffered a rapid orbital decay to the center due to dynamical friction in one Hubble time, forming a nucleated dwarf galaxy. For instance, under the assumption that mass follows light or assuming a NFW profile, Fornax GCs 3 and 4, which are at distances to the center  $< 0.6 \text{ kpc}$ , should have decayed to the center of Fornax in  $\sim 0.5\text{--}1 \text{ Gyr}$  [41, 42] (see also Fig. 7 in [65]); this clearly represents a timing problem. Assuming a cuspy NFW halo with the same parameters as those reported in [65], GCs 1, 2, 3 and 5 can remain in orbit as long as their starting distances from Fornax center are  $\gtrsim 1.6 \text{ kpc}$ , whereas GC 4 needs an initial distance  $\gtrsim 1.2 \text{ kpc}$ . However, there is no statistical evidence to suggest that the initial distribution of GCs is so different to the stellar background distribution. Lotz et al. [66] found that the summed distribution of the entire GC systems in 51 Virgo and Fornax cluster dwarf ellipticals closely follows the exponential profile of the underlying stellar population.

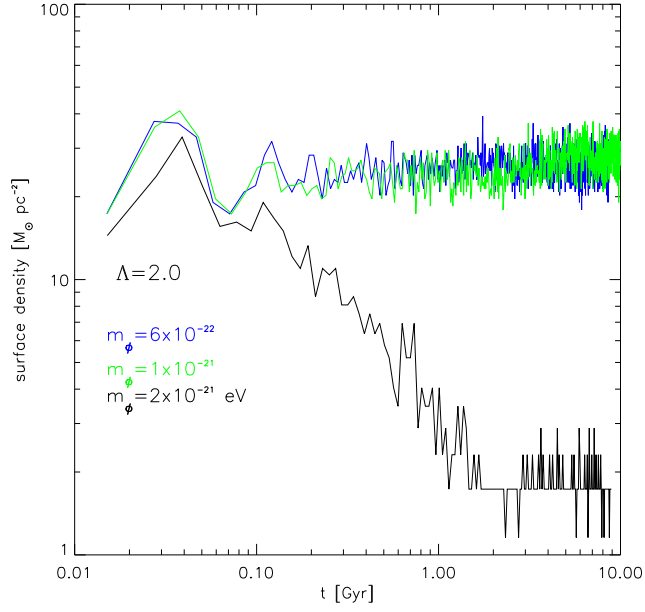


**Figure 8.** Same as figure 7 but for  $\Lambda = 2.0$ .

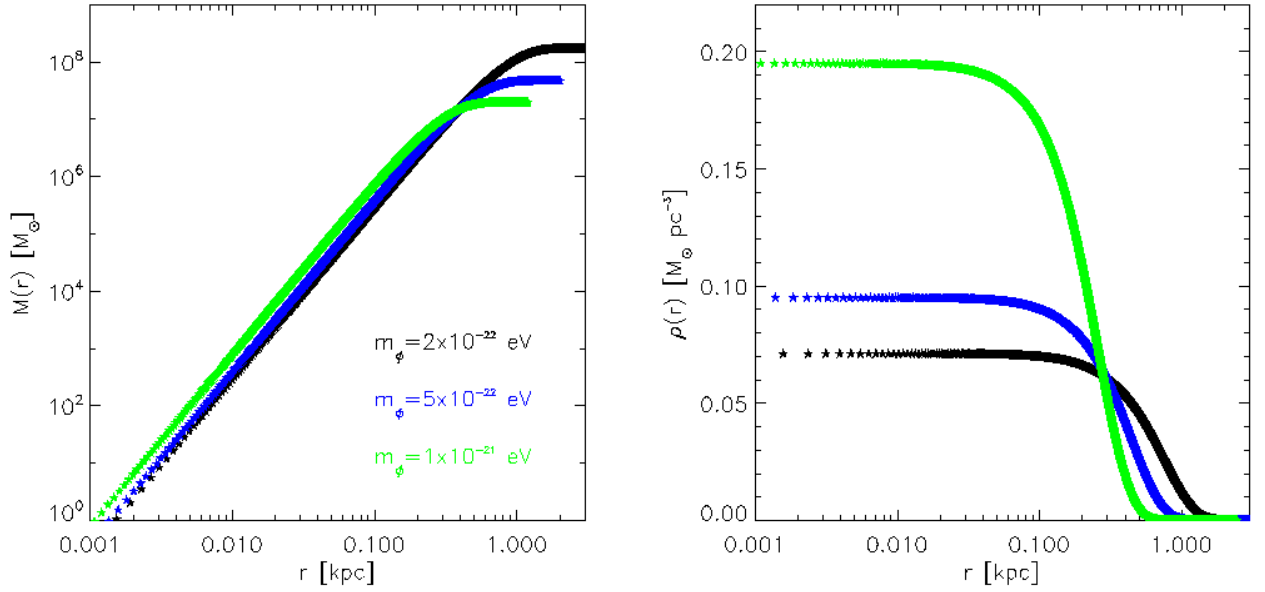


**Figure 9.** Mass interior to any given radius and density profiles for SFDM halos for models with  $\Lambda = 1/2$  and different  $m_\phi$ .

In addition, studies of the radial distribution of GCs in giant elliptical galaxies show that the distribution of metal-rich GCs matches the galaxy light distribution [67, 68]. Assuming that GCs formed along with the bulk of the field star population in dwarf galaxies, the probability that Fornax GCs were formed all beyond 1.2 kpc is  $\sim (0.03)^5 \simeq 2.5 \times 10^{-8}$  (here we have

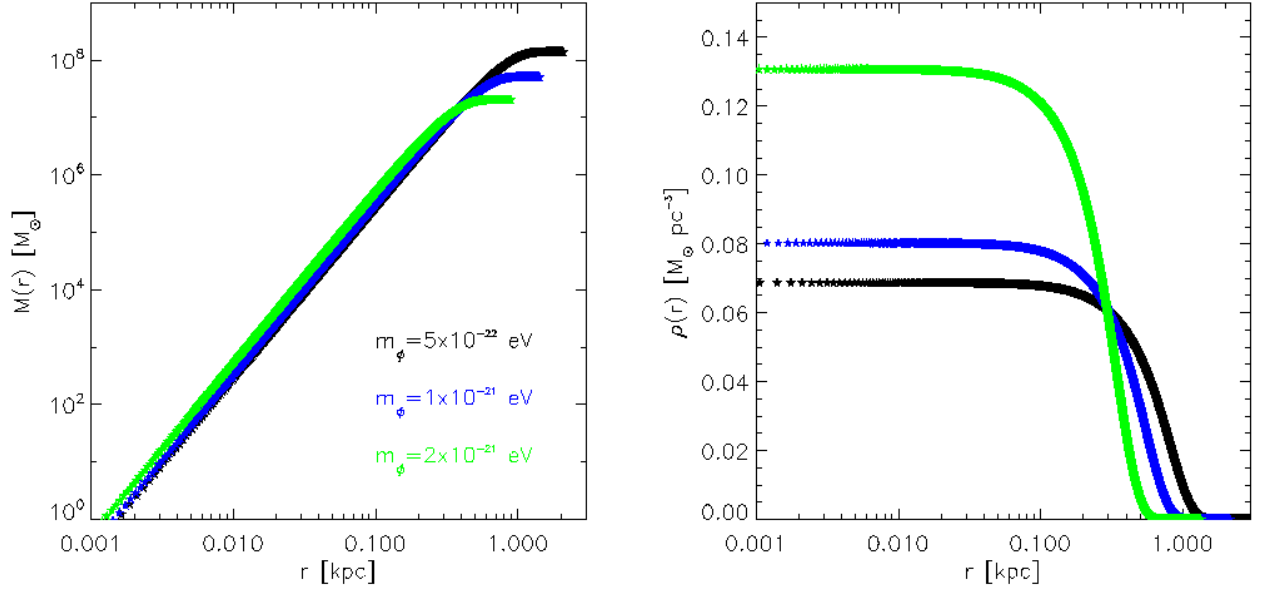


**Figure 10.** Mass interior to any given radius and density profiles for SFDM halos for models with  $\Lambda = 2$  and different  $m_\phi$ .

**Table 2.** Same as Table 1 but for models with small self-interaction parameter.

$\Lambda$	$m_\phi$ ( $10^{-22}\text{eV}$ )	$\epsilon$ ( $10^{-5}$ )	$M$ ( $10^7 M_\odot$ )	$r_{95}$ (kpc)	$r_c$ (kpc)	destruction time (Gyr)
0.5	2.	8.13	17.13	1.57	0.62	$> 10$
0.5	5.	5.53	4.66	0.92	0.36	$\sim 5$
0.5	10.	4.68	2.0	0.55	0.22	$\sim 0.4$
2.0	2.	7.9	53.27	1.95	1.06	$> 10$
2.0	5.	5.1	13.73	1.21	0.66	$> 10$
2.0	10.	3.75	5.05	0.82	0.45	$> 10$
2.0	20.	3.0	2.02	0.51	0.28	$\sim 1.0$

used that the fraction of the stellar mass beyond 1.2 kpc for a King model with a core radius of 0.4 kpc and a concentration parameter of 0.72, as used in [65], is less than 3 percent). Therefore, it is very unlikely that all the GCs in Fornax were formed at such large distances and even they did, there is still a timing problem with GCs 3 and 4.

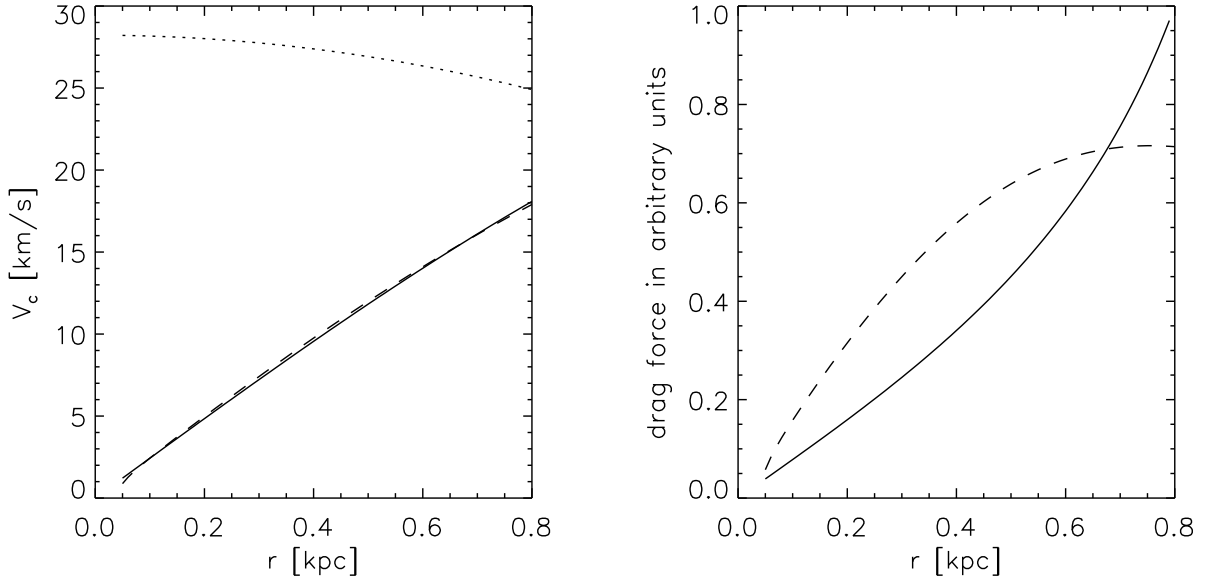


**Figure 11.** Left panel: Circular velocity (solid line) and sound speed (dotted line) as a function of galactocentric distance for a SFDM model with  $m_\phi^4/\lambda = 0.55 \times 10^3 \text{ eV}^4$  and  $R_{\text{max}} = 2.1 \text{ kpc}$ . For comparison we also plot the circular velocity in the cored collisionless DM halo employed by Sánchez-Salcedo et al. [42] to solve the problem of orbit surviving. Right panel: Gravitational drag force in these models. Solid line stands for the SFDM model and dashed line for the the cored collisionless halo.

The dynamical friction timescale depends on the nature of DM particles. Goodman [69] was the first to suggest that the suppression of dynamical friction in superfluid DM halos could circumvent some problems in galactic dynamics such as the presence of rotating bars in dense dark halos (see also [70, 71]). Here we will study if SFDM halos can solve or alleviate the timing problem of the GCs in dwarf galaxies.

We consider first the so-called Thomas-Fermi regime, that is, the limit of large scattering parameter ( $\Lambda \gg 1$ ). In this limit, the dynamics of the scalar field is effectively the same as that for an ideal fluid with equation of state  $P = K\rho^2$  and  $K = \lambda/m_\phi^4$  (see [71] and the Appendix). Therefore, the SFDM dynamical friction force exerted on a gravitational object is the same as it is in a gaseous medium with sound speed  $c_s = (2K\rho)^{1/2}$  (see the Appendix).

Ostriker [72] calculated the drag force on a perturbing body of mass  $M_p$  moving at constant speed  $V_0$  through an ideal fluid with sound speed  $c_s$ . She found that for subsonic perturbers, that is  $\mathcal{M} < 1$  where the Mach number is defined as  $\mathcal{M} \equiv V_0/c_s$ , the drag force is generally smaller in a gaseous medium than in a collisionless medium, because pressure forces in a gaseous medium create a symmetric distribution in the vicinity of the perturber. More specifically, she found that at  $\mathcal{M} < 1$  the dynamical friction force  $F_{DF}$  in a gaseous and homogeneous medium is

$$F_{DF} = \frac{4\pi(GM_p)^2\rho_0}{V_0^2} \left[ \frac{1}{2} \ln \left( \frac{1+\mathcal{M}}{1-\mathcal{M}} \right) - \mathcal{M} \right], \quad (4.1)$$

where  $\rho_0$  is the unperturbed fluid density. Moreover, Kim & Kim [73] demonstrated that Ostriker’s formula for the subsonic case, which was derived for perturbers in rectilinear orbits,



is also valid for objects on circular orbits.

We consider now the decay of GCs on near-circular orbits in a spherical self-gravitating halo of fluid DM with polytropic index  $\gamma = 2$ , due to dynamical friction. In that halo, the circular speed depends on the galactocentric distance  $r$ ,  $V_0(r) = \sqrt{GM(r)/r}$ , where  $M(r)$  is given in Eq. (3.3). The motion is subsonic, i.e.  $V_0/c_s < 1$ , at any radius interior to  $0.84r_c$ . Figure 11 shows the halo circular velocity, sound speed and the drag force (using Eq. 4.1) as a function of the distance to the center of Fornax for a model with  $R_{\text{max}} = 2.1$  kpc, which corresponds to  $r_c = 1.25$  kpc and  $m_\phi^4/\lambda = 0.55 \times 10^3 \text{ eV}^4$ . For comparison, we also plot the corresponding curves for a King halo made of collisionless particles with a core large enough to solve the timing problem in Fornax (see [42] for details). Within a galactocentric distance of 0.8 kpc, the dynamical friction in a collisionless halo with a King radius of 1.5 kpc is similar to the drag force in a SFDM halo with a core radius of 1.25 kpc and thus, conclude that models with  $m_\phi^4/\lambda \lesssim 0.55 \times 10^3 \text{ eV}^4$  are compatible with the radial distribution of the population of GCs in Fornax.

In the noninteracting case, the equation governing the evolution of the perturbation is no longer a wave equation with constant sound speed but, instead, the velocity group depends on the wavenumber [74]. The derivation of the steady density wake in a homogeneous medium is outlined in the Appendix. For a perturber moving at speed  $V_0$  in rectilinear orbit along the  $z$ -axis, it is convenient to define the transonic wavenumber as  $k_0 \equiv m_\phi V_0/\hbar$  and the radial wavenumber  $k_R^2 = k_x^2 + k_y^2$ . In the Appendix, we show that Fourier modes with radial wavenumber  $k_R$  larger than  $k_0$  behaves subsonically, whereas modes with  $k_R < k_0$  are supersonic. Consider a GC on circular orbit with radius  $R_{\text{orb}} = 0.8$  kpc from the galactic center of Fornax with a circular velocity  $\simeq 18 \text{ km s}^{-1}$  (see Fig. 11). For  $m_\phi = (0.1 - 1) \times 10^{-22} \text{ eV}$ , the transonic wavenumber is  $k_0 = 0.1 - 1 \text{ kpc}^{-1}$ . Small  $k_0$  values imply that the motion is supersonic only for Fourier modes with large wavelength. Since GCs are assumed to be on quasicircular orbits, the direction of  $\mathbf{V}_0$  changes by  $\pi/2$  four times per orbit and thus the forward-wave propagation effectively restarts as well [72, 73, 75]. This implies that modes with wavelength much larger than  $R_{\text{orb}}$  are not relevant. In fact, because the wake bends behind the body, the drag force promptly saturates to a steady-state value within less than the crossing time of modes over the distance equal to the orbital diameter [73]. Therefore, we may state that the perturber is essentially subsonic provided that  $k_0^{-1} \gtrsim R_{\text{orb}}$ . As dynamical friction is effectively suppressed for subsonic perturbers, Fornax GCs within a radius of  $\sim 1$  kpc are expected to avoid significant orbital decay if  $k_0 \lesssim 1 \text{ kpc}^{-1}$ , which implies  $m_\phi < 1 \times 10^{-22} \text{ eV}$ . Thus,  $m_\phi$  values between  $0.3 \times 10^{-22} \text{ eV}$  and  $1 \times 10^{-22} \text{ eV}$  could explain the survival of the dynamical fossil in UMi and may alleviate the timing problem of the GCs orbiting dwarf galaxies.

## 5 Concluding Remarks

We have considered a model where ultra-light bosons are the main components of the dark halos of galaxies. The main goal of this work was to constrain the mass of the scalar particles. We constructed stable equilibrium configurations of SFDM in the Newtonian limit to model the DM halo in UMi. We studied two relevant cases of SFDM halos: with and without self-interaction.

The persistence of cold substructures in UMi places upper limits on  $m_\phi$ . Using  $N$ -body simulations, we found that the survival of cold substructures in UMi is only possible if  $m_\phi < 3 \times 10^{-22} \text{ eV}$  in the  $\Lambda = 0$  case. On the other hand, by imposing a plausible upper

**Table 3.** Relevant parameters of the halo for models with large self-interaction.

$R_{max}$ (kpc)	$m_\phi^4/\lambda$ ( $10^3 \text{ eV}^4$ )	$\phi_c^2$ ( $10^{-9}$ )	$r_c$ (kpc)	$M$ ( $10^8 \text{ M}_\odot$ )
1.2	1.7	6.35	0.72	1.6
1.3	1.4	7.35	0.78	2.0
1.4	1.2	8.4	0.84	2.5
1.5	1.1	9.6	0.90	3.0
1.6	0.94	10.8	0.96	3.6
1.7	0.83	12.1	1.02	4.3
1.8	0.74	13.5	1.08	5.1

limit on  $M$ , we place lower limits on  $m_\phi$ . All together, we find that for  $\Lambda = 0$ ,  $m_\phi$  should be in the window

$$0.3 \times 10^{-22} \text{ eV} < m_\phi < 3 \times 10^{-22} \text{ eV}. \quad (5.1)$$

Since the timing problem of the orbital decay of the GCs in Fornax can be alleviated if  $m_\phi < 1 \times 10^{-22} \text{ eV}$  for  $\Lambda = 0$ , our most favored value is around  $(0.3 - 1) \times 10^{-22} \text{ eV}$ .

For SFDM models with self-interaction, the upper limit on  $m_\phi$  increases with  $\Lambda$ . For  $\Lambda = 2$ , halos made up by bosons of mass  $\lesssim 6 \times 10^{-22} \text{ eV}$  could account for the observed internal dynamics of UMi. In the limit  $\Lambda \gg 1$ , we find that  $m_\phi^4/\lambda \lesssim 0.55 \times 10^3 \text{ eV}^4$  would explain the longevity of UMi's clump and the surviving problem of GCs in Fornax.

The window of permitted values for  $m_\phi$  is quite narrow. Even so, it is remarkable that our preferred range for the mass of the boson derived from the dynamics of dSph galaxies is compatible with those given by other authors to ameliorate the problem of overabundance of substructure and is consistent with the CMB radiation [10, 13, 23].

In a recent posting during the course of submitting this paper, Slepian and Goodman [71] constrain the mass of bosonic DM using rotation curves of galaxies and Bullet Cluster measurements of the scattering cross section of self-interacting DM (non bosonic) under the assumption that these systems are in thermodynamic equilibrium. If their assumptions are confirmed to be valid, repulsive bosonic DM will be excluded and, thereby, the only remaining window open is non-interacting bosons with masses in the range given in equation (5.1). Nevertheless, the static diffusive equilibrium between Bose-Einstein condensate and its non-condensated envelope, as well as finite temperature effects need to be reconsidered [76]. In addition, other authors [63, 77] argue that scattering cross sections for bosonic DM are much smaller than those derived from the condition of thermodynamic equilibrium by Slepian and Goodman [71].

## 6 Acknowledgments

The authors wish to thank the referee for useful comments. V.L. gratefully acknowledges support from the Alexander von Humboldt Foundation fellowship and Stu group. A.B. acknowledges CONACyT postdoctoral grant. This work was partially supported by CONACyT under grant 60526 and by DGAPA-UNAM under grant IN115311. This is part of the Instituto Avanzado de Cosmología (IAC) collaboration.

## A Wake created by a gravitational perturber in an infinite homogeneous medium

In order to derive the dynamical friction felt by a gravitational perturber moving through a SFDM medium or Bose-Einstein condensate, it is convenient to use the hydrodynamical representation [74, 78]. In the quantum-mechanical equation of motion (2.1), we write the wave function in the form  $\psi(\mathbf{r}, t) = A(\mathbf{r}, t) \exp(iS(\mathbf{r}, t)/\hbar)$  where  $A$  and  $S$  are real functions, and make the Madelung transformation  $\rho = m_\phi^2 |\psi|^2 = m_\phi^2 A^2$  and  $\mathbf{v} = \nabla S/m_\phi$ , to find

$$\frac{\partial \rho}{\partial t} + \nabla(\rho \cdot \mathbf{v}) = 0, \quad (\text{A.1})$$

$$\frac{\partial \mathbf{v}}{\partial t} + (\mathbf{v} \cdot \nabla) \mathbf{v} = -\nabla(U + U_{\text{ext}} + Q) - \frac{1}{\rho} \nabla P_s, \quad (\text{A.2})$$

where  $P_s$  is the pressure arising from the short-range interactions,  $U_{\text{ext}}$  is the moving and rigid gravitational potential created by the perturber (a GC in our case) and

$$Q = -\frac{\hbar^2}{2m_\phi^2 \sqrt{\rho}} \nabla^2 \sqrt{\rho} \quad (\text{A.3})$$

is the quantum potential, which arises from the Heisenberg uncertainty principle. The equation of state is polytropic,  $P_s = K\rho^\gamma$ , with index  $\gamma = 2$  and  $K = \lambda/(4m_\phi^4)$  [69, 74]. Thus, we can define the sound speed as  $c_s = (2K\rho)^{1/2}$ .

The Thomas-Fermi approximation amounts to neglecting the quantum potential in Eq. (A.2). In that case, Equations (A.1)-(A.2) reduce to the usual Euler equations of a fluid. Therefore, all we know about dynamical friction in gaseous media holds valid for a Bose-Einstein condensate.

In the noninteracting case, the particles interact only via gravity and thus  $P_s = 0$ . We study the completely steady flow created by a gravitational perturber moving in a straight-line trajectory at constant-speed  $\mathbf{V}_0$  through a homogeneous (infinite) medium. The gravitational attraction between the perturber and its own wake is the dynamical friction force. Consider a particle at the origin of our coordinate system, surrounded by a scalar field medium whose velocity far from the particle is  $\mathbf{V}_0 = -V_0 \hat{\mathbf{z}}$ , with  $V_0 > 0$ . We will assume that the perturber induces a small perturbation and hence describe the medium's response in linear theory. Once linearized, the quantum Euler equations (A.1)-(A.2) with  $P_s = 0$  are

$$\rho_0 \nabla \cdot \mathbf{v}' + \mathbf{V}_0 \cdot \nabla \rho' = 0, \quad (\text{A.4})$$

$$\mathbf{V}_0 \cdot \nabla \mathbf{v}' = -\nabla U_{\text{ext}} + \frac{\hbar^2}{4m_\phi^2} \nabla \left[ \nabla^2 \frac{\rho'}{\rho_0} \right], \quad (\text{A.5})$$

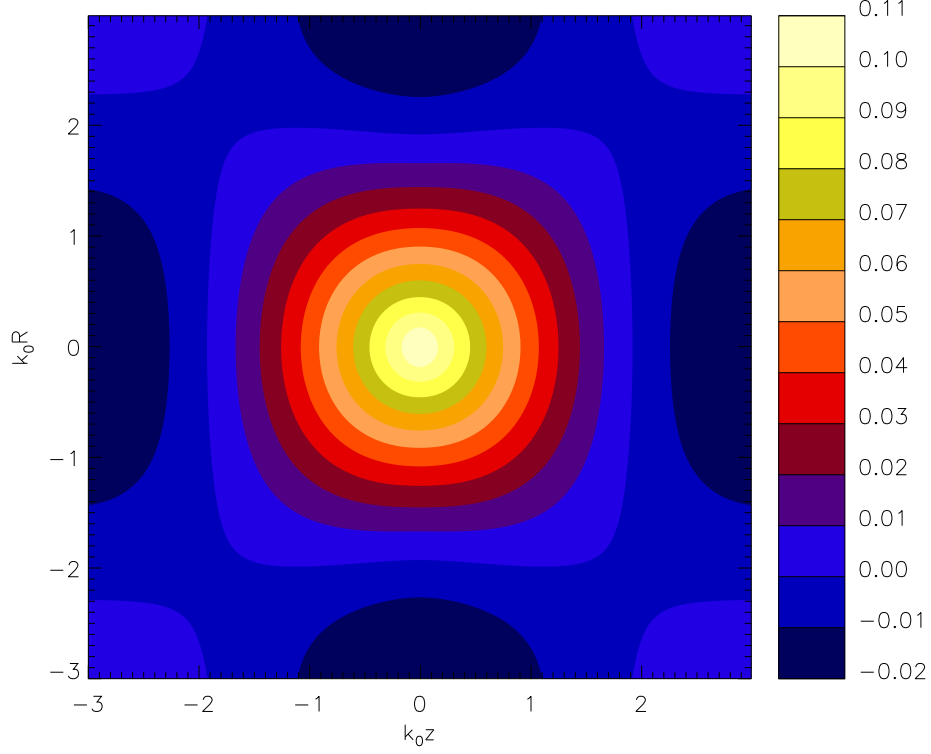


**Figure 12.** Map of  $\xi_{\text{II}}$ . Note that this is a dimensionless quantity that describes the front-back symmetric part of the perturbed density in units of  $GM_p k_0 \rho_0 / V_0^2$ .

where  $\rho' = \rho - \rho_0$  and  $\mathbf{v}' = \mathbf{v} - \mathbf{V}_0$ . By substituting Eq. (A.4) into the divergence of Eq. (A.5), we find a single differential equation for the density perturbation,  $\alpha \equiv \rho' / \rho_0$ ,

$$-V_0^2 \frac{\partial^2 \alpha}{\partial z^2} = -\nabla^2 U_{\text{ext}} + \frac{\hbar^2}{4m_\phi^2} \nabla^2 [\nabla^2 \alpha], \quad (\text{A.6})$$

which is a three dimensional version of the Bernoulli-Euler beam equation. For a point-mass  $M_p$ , we have that  $\rho_{\text{ext}} = M_p \delta(x) \delta(y) \delta(z)$  and, hence,  $\nabla^2 U_{\text{ext}} = 4\pi G M_p \delta(x) \delta(y) \delta(z)$ . Taking the Fourier transform of Equation (A.6), we have

$$\frac{\hbar^2}{4m_\phi^2} (k^4 - 4k_0^2 k_z^2) \hat{\alpha} = \sqrt{\frac{2}{\pi}} G M_p, \quad (\text{A.7})$$

where  $k_0 \equiv m_\phi V_0 / \hbar$ . The density perturbation is recovered by doing the inverse Fourier transform,

$$\alpha(\mathbf{r}) = \frac{2G M_p m_\phi^2}{\pi^2 \hbar^2} \int \frac{\exp(i\mathbf{k} \cdot \mathbf{r})}{k^4 - 4k_0^2 k_z^2} d^3 \mathbf{k}. \quad (\text{A.8})$$

In order to find the poles of the integrand, it is convenient to write the above equation as

$$\alpha(\mathbf{r}) = \frac{2GM_p m_\phi^2}{\pi^2 \hbar^2} \int \frac{\exp(i\mathbf{k} \cdot \mathbf{r})}{(k_z^2 - \chi_+^2)(k_z^2 - \chi_-^2)} d^3\mathbf{k}, \quad (\text{A.9})$$

where  $\chi_\pm = k_0 \pm \sqrt{k_0^2 - k_R^2}$  and  $k_R^2 = k_x^2 + k_y^2$ . The integral (A.9) along  $k_z$  is evaluated by transforming to the complex plane. For  $k_R > k_0$ , all the poles are outside the contour of integration, whereas the integrand has poles on the real axis for  $k_R < k_0$ . This reflects the fact that Fourier modes with  $k_R > k_0$  has a velocity group larger than the perturber's velocity and thus are supersonic, whereas modes with small wavenumber ( $k_R < k_0$ ) are subsonic<sup>1</sup>. It is convenient to subdivide the interval of integration over  $k_R$  into two parts:  $[0, k_0]$  (interval I) and  $[k_0, \infty]$  (interval II). Thus  $\alpha(\mathbf{r}) = \alpha_I(\mathbf{r}) + \alpha_{II}(\mathbf{r})$ , where  $\alpha_I(\mathbf{r})$  corresponds to the  $k_R$ -integral over interval I and  $\alpha_{II}(\mathbf{r})$  is the integral over interval II. The component  $\alpha_{II}(\mathbf{r})$  displays front-back symmetry, whereas the contribution  $\alpha_I(\mathbf{r})$  is nonzero only behind the body in order to preserve causality. In terms of the dimensionless distance along the symmetry axis  $\tilde{z} \equiv k_0 z$ , and the dimensionless cylindrical radius  $\tilde{R} \equiv k_0 R$ , the density perturbation can be written as

$$\alpha(\tilde{z}, \tilde{R}) = \frac{GM_p k_0}{V_0^2} \left[ \xi_I(\tilde{z}, \tilde{R}) + \xi_{II}(\tilde{z}, \tilde{R}) \right], \quad (\text{A.10})$$

where  $\xi_I(\tilde{z}, \tilde{R})$  and  $\xi_{II}(\tilde{z}, \tilde{R})$  are dimensionless quantities, and the subscripts I and II refer to the asymmetric and the symmetric parts, respectively. We see that the density enhancement at  $(\tilde{z}, \tilde{R})$  decreases with increasing  $V_0$  and increases with  $k_0$ .

For illustration, the symmetric part of the density perturbation,  $\xi_{II}$ , is shown in Figure 12. This map represents the symmetric contribution of the steady-state density perturbation created by a gravitational perturber moving in an infinite homogeneous medium. We see that the density isocontours are extremely spherical (for a comparison with the isocontours in a gaseous medium see [72]). The time-dependent evolution of the wake generated by, and the gravitational drag force on, a body traveling on a circular orbit will be presented in a forthcoming paper.

## References

- [1] Klypin, A., Kravtsov, A., Valenzuela, O. & Prada, F., *Where Are the Missing Galactic Satellites?*, *Astrophys. J.* 522 (1999) 82 [astro-ph/9901240].
- [2] Ostriker, J. P., & Steinhardt, P., *New Light on Dark Matter*, *Science* 300 (2003) 1909 [astro-ph/0306402].
- [3] van den Bosch, F. C., Robertson, B. E., Dalcanton, J. J. & de Blok, W. J. G., *Constraints on the Structure of Dark Matter Halos from the Rotation Curves of Low Surface Brightness Galaxies*, *Astron. J.* 119 (2000) 1579 [astro-ph/9911372].
- [4] Kleyna, J. T., Wilkinson, M. I., Gilmore, G. & Evans, N. W., *A Dynamical Fossil in the Ursa Minor Dwarf Spheroidal Galaxy*, *Astrophys. J.* 588 (2003) L21 [astro-ph/0304093].
- [5] de Blok, W. J. G. & Bosma, A., *High-resolution rotation curves of low surface brightness galaxies*, *Astron. and Astrophys.* 385 (2002) 816 [astro-ph/0201276].
- [6] Sin S.J., *Late-time phase transition and the galactic halo as a Bose liquid*, *Phys. Rev. D* 50 (1994) 3650 [hep-ph/9205208].

---

<sup>1</sup>See [74] for the derivation of the velocity group.

- [7] Peebles, P.J.E., & Vilenkin, A., *Noninteracting dark matter*, *Phys. Rev. D.* 103506 (1999) 60 [astro-ph/9904396].
- [8] Peebles, P.J.E., *Fluid dark matter*, *Astrophys. J.* L127 (1999) 543 [astro-ph/9904396].
- [9] Sahni, V. and Wang, L., *New cosmological model of quintessence and dark matter*, *Phys. Rev. D* 62 (2000) 103517 [astro-ph/9910097].
- [10] Hu W., Barkana, R., & Gruzinov A., *Fuzzy Cold Dark Matter: The Wave Properties of Ultralight Particles*, *Phys. Rev. Lett.* 85 (2000) 1158 [astro-ph/0003365].
- [11] Matos, T., Guzmán F. S. & Ureña-Lopez, L. A., *Scalar field as dark matter in the universe*, *Class. Quant. Grav.* 17 (2000) 1707 [astro-ph/9908152].
- [12] Matos, Ureña-Lopez, L. A., *LETTER TO THE EDITOR: Quintessence and scalar dark matter in the Universe*, *Class. Quant. Grav.* 17 (2000) L75 [astro-ph/0004332].
- [13] Matos, T., & Ureña-Lopez, L. A., *Further analysis of a cosmological model with quintessence and scalar dark matter*, *Phys. Rev. D* 63 (2001) 063506 [astro-ph/0006024].
- [14] Arbey A., Lesgourgues, J., & Salati, P., *Quintessential halos around galaxies*, *Phys. Rev. D* 64 (2001) 123528 [astro-ph/0105564].
- [15] Lee, Jae-Weon, *Is Dark Matter a BEC or Scalar Field?*, *J. Korean Phys.Soc.* 54 (2009) 2622 [arXiv:0801.1442].
- [16] Marsh, D.J.E., & Ferreira, P. G., *Ultra-Light Scalar Fields and the Growth of Structure in the Universe*, *Phys. Rev. D.* 82 (2010) 103528 [astro-ph/0812.1342v3].
- [17] Ureña-López, L. A., *Bose-Einstein condensation of relativistic Scalar Field Dark Matter*, *J. Cosmol. Astropart. Phys.* JCAP01(2009)014 [gr-qc/0806.3093].
- [18] Lundgren, A.P., Bondarescu, M., Bondarescu, R., & Balakrishna, J., *Lukewarm dark matter: Bose condensation of ultralight particles*, *Astrophys. J.* 715 (2010) L35 [astro-ph/1001.0051v2].
- [19] Hwang, J. C, *Roles of a coherent scalar field on the evolution of cosmic structures*, *Phys. Lett. B* 401 (1997) 241 [astro-ph/9610042].
- [20] Matos, T. & Suárez, A., *Structure formation with scalar-field dark matter: the fluid approach*, *Mon. Not. Roy. Astron. Soc.* 416 (2011) 87 [arXiv:1101.4039].
- [21] Turner, M. S. *Coherent scalar-field oscillations in an expanding universe*, *Phys. Rev. D* 28 (1983) 1243.
- [22] Matos, T., Vázquez-González, A., & Magaña, J.,  $\phi^2$  as dark matter, *Mon. Not. Roy. Astron. Soc.* 393 (2009) 1359 [astro-ph/0806.0683].
- [23] Rodríguez-Montoya, I., Magaña, J., Matos, T., & Pérez-Lorezana, A., *Ultra Light Bosonic Dark Matter and Cosmic Microwave Background*, *Astrophys. J.* 721 (2010) 1509 [arXiv:0908.0054].
- [24] Chavanis, P.H. *Mass-radius relation of Newtonian self-gravitating Bose-Einstein condensates with short-range interactions. II. Numerical results*, *Phys. Rev. D* 84 (2011) 043532, [arXiv:1103.1103.2054].
- [25] Gleiser, M., *Stability of boson stars*, *Phys. Rev. D.* 38 (1988) 2376.
- [26] Lee, T.D., & Yang Pang, *Stability of mini-boson stars*, *Nuclear Physics B* 315 (1988) 477.
- [27] Kusmartsev, F.V., Mielke, E.W., & Schunk, F.E., *Stability of neutron and boson stars: a new approach based on catastrophe theory*, *Phys. Lett. A* 157 (1991) 465.
- [28] Seidel, E., & Suen Wai-Mo, *Dynamical evolution of boson stars: perturbing the ground state*, *Phys. Rev. D.* 42 (1990) 384.
- [29] Jetzer, P., *Boson stars*, *Phys. Reports* 220 (1992) 163.



- [30] Balakrishna, J., Bondarescu, R., Daues, G., Guzman F.S., Seidel, E., *Evolution of 3D Boson Stars with Waveform Extraction*, *Class. Quant. Grav.* 23 (2006) 2631.
- [31] Bernal, A., & Guzmán, F. S., *Scalar field dark matter: Nonspherical collapse and late-time behavior*, *Phys. Rev. D* 74 (2006) 063504 [astro-ph/0608523].
- [32] Ji S. U., & Sin Sang-Jin, *Late-time phase transition and the galactic halo as a Bose liquid. II. The effect of visible matter*, *Phys. Rev. D* 50 (1994) 3655 [arXiv:hep-ph/9409267].
- [33] Bernal, A., Matos T., & Núñez, D., *Flat Central Density Profiles from Scalar Field Dark Matter Halos*, *Rev. Mex. Astron. Astrof.* 44 (2008) 149 [astro-ph/0303455].
- [34] Jae-Weon Lee, & Sooil Lim, *Minimum mass of galaxies from BEC or scalar field dark matter*, *JCAP* 1001 (2010) 007 [astro-ph/0812.1342v3].
- [35] Jae-weon Lee & In-guy Koh, *Galactic Halos As Boson Stars*, *Phys. Rev. D.* 53 (1996) 2236 [hep-ph/9507385v2].
- [36] Arbey A., Lesgourgues, J., & Salati, P., *Galactic halos of fluid dark matter*, *Phys. Rev. D* 68 (2003) 023511 [astro-ph/0301533].
- [37] Böhmer, C. G., & Harko, T., *Can dark matter be a Bose Einstein condensate?*, *J. Cosmol. Astropart. Phys.* JCAP06(2007)025 [astro-ph/0705.4158v4].
- [38] Harko, T., *Bose-Einstein condensation of dark matter solves the core/cusp problem*, *J. Cosmol. Astropart. Phys.* JCAP05(2011)022 [arXiv:1105.2996].
- [39] Bernal, A., & Guzmán, F. S., *Scalar field dark matter: Head-on interaction between two structures*, *Phys. Rev. D* 74 (2006) 103002 [astro-ph/0610682].
- [40] Gonzalez, J. A. & Guzmán, F. S., *Interference pattern in the collision of structures in the Bose-Einstein condensate dark matter model: Comparison with fluids*, *Phys. Rev. D* 83 (2011) 103513 [arXiv:1105.2066].
- [41] Goerdt, T., Moore, B., Read, J. I., Stadel, J. & Zemp, M., *Does the Fornax dwarf spheroidal have a central cusp or core?*, *Mon. Not. Roy. Astron. Soc.*, 368 (2006) 1073 [astro-ph/0601404].
- [42] Sánchez-Salcedo, F. J., Reyes-Iturbide, J. & Hernandez, X., *An extensive study of dynamical friction in dwarf galaxies: the role of stars, dark matter, halo profiles and MOND*, *Mon. Not. Roy. Astron. Soc.* 370 (2006) 1829 [astro-ph/0601490].
- [43] Battaglia, G., Helmi, A., Tolstoy, E., Irwin, M., Hill, V. & Jablonka, P., *The Kinematic Status and Mass Content of the Sculptor Dwarf Spheroidal Galaxy*, *Astrophys. J.* 681 (2008) L13 [arXiv:0802.4220].
- [44] Amorisco, N. C. & Evans, N. W., *Dark Matter Cores and Cusps: The Case of Multiple Stellar Populations in Dwarf Spheroidals*, 2011, [arXiv:1106.1062v1].
- [45] Gilmore, G., Wilkinson, M. I., Wyse, R. F. G., Kleyna, J. T., Koch, A., Evans, N. W & Grebel, E. K., *The Observed Properties of Dark Matter on Small Spatial Scales*, *Astrophys. J.* 663 (2007) 948 [astro-ph/0703308v1].
- [46] Friedberg, R., Lee, T.D., & Pang, Y., *Mini-soliton stars*, *Phys. Rev. D* 35 (1987) 3640.
- [47] Chi-Wai Lai PhD Thesis. <http://laplace.phas.ubc.ca/Members/matt/Doc/Theses/Phd/lai.pdf>
- [48] A. Bernal PhD Thesis. <http://www.fis.cinvestav.mx/thesis/index.php/thesis>
- [49] Guzman, F. Siddhartha & Ureña-López, L. Arturo, *Evolution of the Schrödinger-Newton system for a self-gravitating scalar field*, *Phys. Rev. D* 69 (2004) 124033 [gr-qc/0404014].
- [50] Grebel, E. K., Gallagher, J. S., Harbeck, D., *The Progenitors of Dwarf Spheroidal Galaxies*, *Astronomical. J* 125 (2003) 1926
- [51] Lora, V., Sánchez-Salcedo, F. J., Raga, A. C. & Esquivel, A., *An Upper Limit on the Mass of*



- the Black Hole in Ursa Minor Dwarf Galaxy*, *Astrophys. J.* 699 (2009) L113 [arXiv:0906.0951].
- [52] Kleyna, J. T., Geller, M. J., Kenyon, S. J., Kutz, M. J., Thorstensen, J. R., *A V and I CCD Mosaic Survey of the Ursa Minor Dwarf Spheroidal Galaxy*, *Astrophys. J.* 115 (1998) 2359.
  - [53] Read, J. I., Wilkinson, M. I., Evans, N. W., Gilmore, G., Kleyna, J. T., *The importance of tides for the Local Group dwarf spheroidals*, *Mon. Not. Roy. Astron. Soc.* 367 (2006) 387 [astro-ph/0511759].
  - [54] Strigari, L. E., Bullock, J. S., Kaplinghat, M., Diemand, J., Kuhlen, K & Madau, P., *Redefining the Missing Satellites Problem*, *Astrophys. J.* 669 (2007) 676 [arXiv:0704.1817].
  - [55] Strigari, L. E., Bullock, J. S., Kaplinghat, M., Simon, J. D., Geha, M., Willman, B., Walker, M. G., *A common mass scale for satellite galaxies of the Milky Way*, *Nature* 454 (2008) 1096 [arXiv:0808.3772].
  - [56] Wilkinson, M. I., Kleyna, J. T., Evans, N. W., Gilmore, G. F., Irwin, M. J., Grebel, E. K., *Kinematically Cold Populations at Large Radii in the Draco and Ursa Minor Dwarf Spheroidal Galaxies*, *Astrophys. J.* 611 (2004) 21 [arXiv:astro-ph/0406520].
  - [57] Peñarrubia, J., McConnachie, A. W., Navarro, J. F., *The Cold Dark Matter Halos of Local Group Dwarf Spheroidals*, *Astrophys. J.* 672 (2008) 90 [arXiv:astro-ph/0701780].
  - [58] Walker, M. G., Mateo, M., Olszewski, E. W., Peñarrubia, J., Wyn E. N., Gilmore, G., *A Universal Mass Profile for Dwarf Spheroidal Galaxies?*, *Astrophys. J.* 704 (2009) 1274 [arXiv:0906.0341].
  - [59] Palma, C., Majewski, S. R., Siegel, M. H., Patterson, R. J., Ostheimer, J. C. & Link, R., *Exploring Halo Substructure with Giant Stars. IV. The Extended Structure of the Ursa Minor Dwarf Spheroidal Galaxy*, *Astron. J.* 125 (2003) 1352 [astro-ph/0205194].
  - [60] Sánchez-Salcedo, F. J., & Lora, V., *Bounds on the Mass and Abundance of Dark Compact Objects and Black Holes in Dwarf Spheroidal Galaxy Halos*, *Astrophys. J.* 658 (2007) L83 [astro-ph/0702502].
  - [61] Strigari, L. E., Bullock, J. S., Kaplinghat, M., Kravtson, A., V., Gnedin, O. Y., *A Large Dark Matter Core in the Fornax Dwarf Spheroidal Galaxy?*, *Astrophys. J.* 652 (2006) 306 [astro-ph/0603775]. Strigari, L. E., Bullock, J. S., Kaplinghat, M., Kravtson, A., V., Gnedin, O. Y., *A Large Dark Matter Core in the Fornax Dwarf Spheroidal Galaxy?*, *Astrophys. J.* 652 (2006) 306 [astro-ph/0603775].
  - [62] Zentner, A. R. & Bullock, J. S., *Halo Substructure and the Power Spectrum*, *Astrophys. J.* 598 (2003) 49 [astro-ph/0304292].
  - [63] Rindler-Daller, T., Shapiro, P. *Angular Momentum and Vortex Formation in Bose-Einstein-Condensed Cold Dark Matter Haloes*, submitted to MNRAS (2011) [arXiv:1106.1256].
  - [64] Colpi, M., Shapiro, S. L., Wasserman, I., *Boson stars - Gravitational equilibria of self-interacting scalar fields*, *Phys. Rev. Lett.* 57 (1986) 2485.
  - [65] Angus, G. W., Diaferio, A. *Resolving the timing problem of the globular clusters orbiting the Fornax dwarf galaxy*, *Mon. Roy. Astron. Soc.* 396 (2010) 887.
  - [66] Lotz, J. M., Telford, R., Ferguson, H. C., Miller, B. W., Stiavelli, M., Mack, J. *Dynamical Friction in DE Globular Cluster Systems*, *Astrophys. J.* 552 (2001) 572
  - [67] Harris, W. E., Petrie, P. L. *The space distribution of globular clusters in M49*, *Astrophys. J.* 223 (1978) 88.
  - [68] Strader, J., Romanowsky, A., Brodie, J., Spitler, L., Beasley, M., Arnold, J., Tamura, N., Sharples, R., Arimoto, N. *Wide-Field Precision Kinematics of the M87 Globular Cluster System*, (2004), [arXiv:1110.2778].

- [69] Goodman, J. *Repulsive dark matter*, *New Astron.* 5 (2000) 103 [arXiv:astro-ph/0003018].
- [70] Goodman, J. & Slepian, Z. *Chance and Chandra*, *Pramana* 77 (2011) 107 [arXiv:1104.2620].
- [71] Slepian, Z., & Goodman, J. *Ruling Out Bosonic Repulsive Dark Matter*, *arXiv:1109.3844*
- [72] Ostriker, E. *Dynamical Friction in a Gaseous Medium*, *Astrophys. J.* 513 (1999) 252 [arXiv:astro-ph/9810324].
- [73] Kim, H. & Kim, W. T. *Dynamical Friction of a Circular-Orbit Perturber in a Gaseous Medium*, *Astrophys. J.* 665 (2007) 432 [arXiv:0705.0084].
- [74] Chavanis, P.H. *Mass-radius relation of Newtonian self-gravitating Bose-Einstein condensates with short-range interactions. I. Analytical results*, *Phys. Rev. D* 84 (2011) 043531, [arXiv:1103.2050].
- [75] Sánchez-Salcedo, F. J., Brandenburg, A. *Dynamical friction of bodies orbiting in a gaseous sphere*, *Mon. Roy. Astron. Soc.* 322 (2001) 67.
- [76] Harko, T., Madarassy, E. J. M. *Finite temperature effects in Bose-Einstein Condensed dark matter halos*, (2011), [arXiv:1110.2829].
- [77] Rodríguez-Montoya I., Pérez-Lorenzana, A., De La Cruz-Burelo, E., Giraud-Héraud, Y., Matos, T. *Cosmic Bose dark matter*, (2011) [arXiv:1110.2751].
- [78] Pitaevskii & Stringari *Bose Einstein Condensation*, (2004), Oxford University Press.